2005

Laser Induced Fluorescence Photobleaching Anemometer for Microfluidic Devices

Guiren Wang
University of South Carolina - Columbia, wanggu@cec.sc.edu

Publication Info

Published in *Lab on a Chip*, Volume 5, Issue 4, 2005, pages 450-456.

Wang, G. R. (2005). Laser induced fluorescence photobleaching anemometer for microfluidic devices. *Lab on a Chip*, 5(4), 450-456.
http://dx.doi.org/10.1039/B416209A

Laser induced fluorescence photobleaching anemometer for microfluidic devices

G. R. Wang

Received 20th October 2004, Accepted 9th February 2005
First published as an Advance Article on the web 4th March 2005
DOI: 10.1039/b416209a

We have developed a novel, non-intrusive fluid velocity measurement method based on photobleaching of a fluorescent dye for microfluidic devices. The residence time of the fluorescent dye in a laser beam depends on the flow velocity and approximately corresponds to the decaying time of the photobleaching of the dye in the laser beam. The residence time is inversely proportional to the flow velocity. The fluorescence intensity increases with the flow velocity due to the decrease of the residence time. A calibration curve between fluorescence intensity and known flow velocity should be obtained first. The calibration relationship is then used to calculate the flow velocity directly from the measured fluorescence intensity signal. The new method can measure the velocity very quickly and is easy to use. It is demonstrated for both pressure driven flow and electroosmotic flow.

Introduction

Microfluidic technology has the potential to significantly change the way modern biology, chemistry, biomedicine and biotechnology are performed and is growing rapidly.[1,2] The corresponding application in biology and chemistry is the so-called Lab-On-a-Chip, which aims at integrating conventional laboratories onto one chip, on which many microscale components are combined. The microfluidic chips enable parallel assays with small samples, high sensitivity and selectivity.

Capillary electrophoresis is often used in microfluidic systems, for example, High Throughput Screening in drug discovery.[3,4] The flow is not only driven by pressure difference, but also by electrokinetic force, *i.e.* electroosmotics and electrophoresis. In order to achieve high throughput, the flow velocity should not be very low and the microchannel for separation should not be very long. Thus, to receive sufficient separation of samples for detection, the pressure difference and electroosmotic flow should be precisely controlled, since the separation time is related to the vector summary of flow velocity of pressure driven flow, electroosmotic flow and electrophoresis.

However, the electroosmotic flow can change during the course of an entire experiment due to the variation of physical or chemical characteristics of a surface, which could result from, for example, protein stickiness on the wall, changes in pH, buffer composition and sample temperature. The change of electroosmotic flow could influence separation quality in electrophoresis in the microfluidic biochips. Possible online or fast monitoring of electroosmotic flow becomes very important when the chip is used for any chemicals that could change surface characteristics, *i.e.* zeta potential.

It is not easy to measure fluid velocity instantaneously with traditional advanced anemometers, such as the Hot Wire Anemometer and Laser Doppler Velocimetry, due to its small size. There are many techniques to measure the velocity or mobility in microchannels for either pressure driven flow or electroosmotic flow. The easiest method to measure the flow velocity is the tracking of neutral markers by measuring the flush time of a neutral marker from injection to detection point.[5–17] Sample weighing[18,19] can measure the velocity, but could be less accurate due to evaporation and sensitivity of the balance. In conductivity cell[20,21] and current monitoring[22–26] average electroosmotic flow (EOF) is measured by observing changes in current and conductivity respectively *versus* time. The velocity can also be determined by measuring streaming potential[27–29] or caged-fluorescence visualization.[30,31] Nuclear magnetic resonance has also been used to measure flow velocity in the research group.[32–35] The most successful method that applies the traditional advanced anemometer, is micro Particle Image Velocimetry (μPIV),[36–38] but it is difficult to apply to commercial instruments. Photobleached Fluorescence Visualization[39–41] and the line writing technique[42–44] with photobleaching are also developed to measure the flow velocity. However, all the methods mentioned above have limited temporal resolution. They can neither measure transient velocity with high temporal and spatial resolution simultaneously, nor be easily used in commercial instruments for online EOF velocity monitoring. Most methods for velocity measurements in electroosmotic flows are referred to in a recent review from Devasenathipathy and Santiago.[45]

The goal of the present work is to develop a diagnostic method that can easily measure transient velocity with potentially high temporal and spatial resolution and make online monitoring of the flow velocity possible in microfluidic devices. We use the name 'Laser-Induced Fluorescence Photobleaching Anemometer' (LIFPA) to describe the flow measurement system detailed in this article. Recently, Wang and Fiedler[46] found that the laser intensity was so high, due to the fine focusing of the laser beam to approximately 4 μm, that the photobleaching became important. Photobleaching resulted in a negative effect for concentration measurements based on LIF, because when flow velocity is sufficiently low, fluorescence intensity depends not only on dye concentration, but

also on the flow velocity. It was suggested that this mechanism could be used to measure flow velocity in a patent.[47] Ricka[48] has qualitatively implemented this method for flow visualization in Benard–Marangoni flow. However, they have not published any flow field measurements. To the author's knowledge, LIFPA has never been used to quantitatively measure flow velocity, nor be used in microfluidic channels, especially for electroosmotic flow.

Theoretical background

The background of this work is based on a simplified model illustrating the relationship between fluorescence intensity and fluid velocity for a given dye concentration due to laser-induced fluorescence photobleaching (LIFP).[46] In the model, fluorescence intensity of the dye increases with fluid velocity at the measuring point due to the LIFP. Such a phenomenon is considered as a negative effect for concentration measurement based on LIF, since we assume that the fluorescence intensity depends only on dye concentration.

However, if we take advantage of such a relationship, LIFP can be used as the theoretical background for the velocity measurement when the dye concentration is a constant.[47] Fig. 1 is a cartoon of the photobleaching process within a laser beam. It is well known that the photobleaching can be described as an exponent decay of fluorescence intensity I_f with time t[49]

$$I_f = I_{f0} \times e^{-t/\tau} \quad (1)$$

where I_{f0} represents fluorescence intensity at $t = 0$; τ denotes the photobleaching time constant, *e.g.* half decay time.

Suppose fluid velocity perpendicular to the laser beam is u, beam width is d_f, and the average dye residence time in the beam is t, then

$$t = d_f/u \quad (2)$$

$$I_f = I_{f0} \times e^{-d_f/(u\tau)} \quad (3)$$

This is the simplified model of the LIFPA, where fluorescence intensity I_f is directly related to flow velocity u. Eqn. (3) indicates that for a given system (dye, buffer, and laser beam property), I_f increases with u. If I_f is known, u can be calculated using eqn. (3). The signal from the optical detector

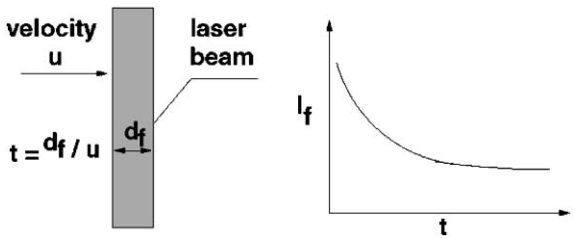

Fig. 1 Cartoon for photobleaching of a dye solution passing through a laser beam in laser-induced fluorescence photobleaching anemometer. The decaying time for the photobleaching is the residence time of the molecular dye in the laser beam.

increases with the total photoemission from the measuring volume. The residence time t of the molecular dye in the laser beam is averaged. Therefore, the smaller the laser beam, the more accurate the model.

In reality, τ, as a system parameter, is dependent of laser intensity at the detecting point, beam width, specific dye and buffer, dye concentration and buffer concentration. Since it is difficult to establish the relationship theoretically, the parameter τ will be determined through experiment. For instance, using several known values of flow velocity u and their corresponding I_f values, we can determine the value of τ. Another useful way is to directly calibrate the relationship between I_f and u. The calibration can be a polynomial curve. With the calibration relation, any instantaneous u can be calculated through the measurement of I_f. The second method is selected in this work.

Experimental section

A Y-channel microfluidic chip microfabricated in fused silica was used for the experiment. The Y-channel chip is 5 cm long, 100 μm wide and 50 μm high. A Harvard syringe pump and a Cole Parmer pump were used to drive syringes containing fluorescence dye solution and pure buffer solution respectively to the microchannel.

The electroosmotic flow was driven by a high voltage supplier 610D from Trek Corporation. Two thin platinum wires 125 μm in diameter that served as electrodes were inserted at the inlet A well and outlet well of the channel, respectively. The inlet A of the channel had high voltage and the outlet was grounded.

Fluorescein sodium salt from Sigma–Aldrich Corporation was used as the dye for the present work. In contrast to conventional fluorescence based diagnostics, the present study desires a fluorescence dye with strong photobleaching property. Since photobleaching can be enhanced with the increase of dye concentration,[46] a high concentration fluorescein dye solution was used in the present study to increase photobleaching. Although fluorescein has high absorption at a wavelength of 488 nm, our test shows that UV light around 337.5–356.40 nm gives stronger photobleaching and higher sensitivity. Note the sensitivity is not the fluorescence intensity, but the slope of the curve of fluorescence intensity to flow velocity. 1 M HEPES solution from Calbiochem Corporation was utilized as buffer and was diluted with DI water to a concentration of 50 mM. The dye was diluted with the same buffer concentration to a concentration of 100 μM. The dye and buffer solution flow into the main channel from different Y-channel inlets respectively, but not simultaneously.

The optical setup is shown in Fig. 2. A Saber Krypton laser from Coherent Corporation was used as the exciting light. The laser power was set to 700 mW for multiline of UV light (337.5–356.40 nm). The laser beam is expanded with a beam expander to 5 mm in diameter and then focused through a cylindrical lens in a sheet with thickness of approximately 25 μm at the detecting point. The beam was projected towards the microchannel at an angle of 45°. The volume corresponding to the spot size is approximately 0.18 nL. A photomultiplier tube H6780–04 from Hamamatsu Corporation

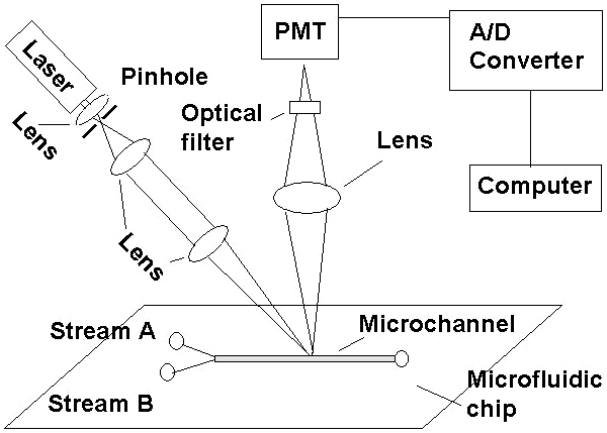

Fig. 2 Schematic of the experimental setup.

was used as an optical detector. An optical band pass filter in the range of 405–475 nm was placed in front of the photomultiplier tube. The signal was recorded as electrical voltage in an Infiniium Oscilloscope, 2 GSa s^{-1}, 4 channels, HP 54825A from Agilent Corporation.

Experimental results

Signal transduction

Our first experiment is to explore whether there exists a measurable signal of fluorescence intensity that is a function of flow velocity, and to verify eqn. (3). The dependence of I_f on u is shown in Fig. 3, where I_f decreases with the reduction of flow rate. Here only one stream of dye solution was used, so that the dye concentration is constant at the detection position. In the initial stage, the flow rate Q was set at 1 μl min^{-1}. After a period of time, the flow and dye concentration in the channel became steady. Then the signal was recorded as a time trace for a period of time, during which, we periodically reduced the flow rate. In Fig. 3, the signal was recorded for 15 s with the flow rate $Q_1 = 1$ μl min^{-1}. During this period, the fluorescence intensity (arbitrary units) was nearly constant at 107.5. As long as the flow rate was kept constant, I_f was also constant. Then the flow rate was switched rapidly to the flow rate of $Q_2 = 0.8$ μl min^{-1}. The signal of fluorescence intensity is then observed to also decrease correspondingly and quickly. This procedure was repeated until Q was reduced to $Q_8 = 0.02$ μl min^{-1} with $I_f = 22.5$. Finally when $Q_9 = 0$ μl min^{-1}, I_f gradually decreased to 2.75. As we know, the flow velocity inside the main channel increases with the flow rate, Fig. 3 clearly displays that I_f increases with u, and this is qualitatively identical to eqn. (3). Fig. 3 shows that the fluorescence intensity increases with flow velocity when other parameters are fixed. Thus, LIFP can be used as signal transduction for flow velocity measurement in a microchannel.

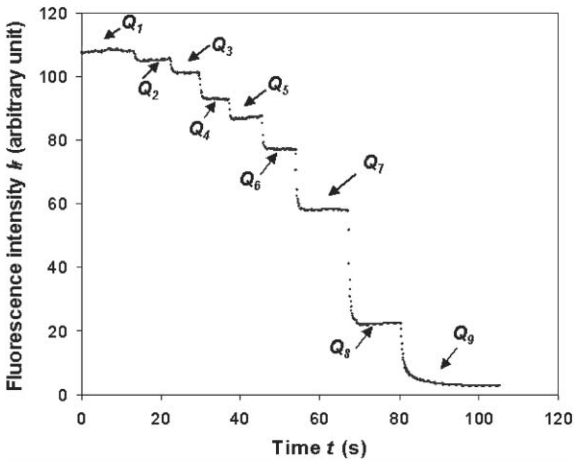

Fig. 3 Time trace of fluorescence intensity with the response to the flow rate change periodically in 9 steps from high flow rate to low flow rate. The flow rate (μl min^{-1}) are: $Q_1 = 1.0$; $Q_2 = 0.80$; $Q_3 = 0.61$; $Q_4 = 0.42$; $Q_5 = 0.30$; $Q_6 = 0.20$; $Q_7 = 0.10$; $Q_8 = 0.020$; $Q_9 = 0$, respectively. The laser power is 700 mW and the measuring spot size is 0.18 nL with focusing beam sheet 25 μm in thickness.

Calibration process

The LIFPA requires calibration between fluid velocity and fluorescence intensity. This means we should first measure the corresponding I_f for each known flow velocity, and then establish a relationship between I_f and u. Such a relation can either be an exponential equation, or even more general, a polynomial, such as

$$u = a_0 + a_1 I_f + a_2 I_f^2 + a_3 I_f^3 + a_4 I_f^4 + a_5 I_f^5 + \ldots \quad (4)$$

We use a polynomial here. For a microfluidic system, the flush time measurement of the sample can be used to determine a steady fluid velocity for a given dye concentration and optical system. The flush time here means the sample migration time from a known injection position to the detection position in the main channel. Either pressure driven flow or EOF can be used for calibration. We used pressure driven flow for the calibration in the present work.

The calibration process is described as follows. For the Y channel, the channel with inlet A supplied dye solution with buffer and the other with inlet B provided pure buffer solution without dye. First, the buffer solution was driven through the main channel with the pump. After the fluorescence signal became steady, the flow was stopped. Next, we pumped the dye solution for less than 1 s and stopped. Then quickly started to pump the buffer solution again in less than 1 s and counted the start time. There was a peak for I_f in the time trace when the dye slug passed through the detecting point. For example, with $Q = 0.1$ μl min^{-1}, we observed the peak at $t = 143$ s as shown in Fig. 4. Due to Taylor dispersion, the time corresponding to the peak was approximately regarded as the flush time. As the channel length is known, the average velocity for a given flow rate setting could be calculated after obtaining the flush time. We obtained the calibrated relationship between I_f and u with filled square symbols shown in Fig. 5 after repeating the same process for several different flow rates.

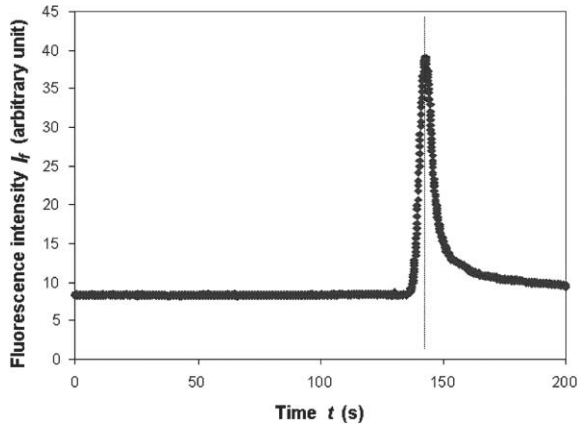

Fig. 4 Fluorescence intensity time trace for flush time measurement. The peak (at t = 143 s) of the signal from the initial low level is an indication of dye solution slug passing through the detecting point. The time trace is used to measure the average migration time of the dye solution slug from the entrance of the main Y channel to the detecting point for average velocity measurement. Because of the Taylor dispersion, the time corresponding to the peak is approximately regarded as the flush time, *i.e.* nearly 143 s.

Based on the calibrated data from Fig. 5, a polynomial for the calibration relation was obtained:

$$u = a_0 + a_1 I_f + a_2 I_f^2 + a_3 I_f^3 + a_4 I_f^4 + a_5 I_f^5$$

$$a_0 = -2.0432472170927346 \times 10^{-1}$$

$$a_1 = 7.6186023325807803 \times 10^{-2}$$

$$a_2 = -5.2267668251621564 \times 10^{-3}$$

$$a_3 = 1.3558472650065237 \times 10^{-4}$$

$$a_4 = -1.4651807110217420 \times 10^{-6}$$

$$a_5 = 5.7832240630262838 \times 10^{-9} \quad (5)$$

Such a relationship is also shown in Fig. 5 as the calibration curve in the non-linear fit line. Therefore the signal of I_f can be used to measure fluid velocity. Fig. 5 shows that at a very low velocity range, the relation between I_f and u can approximately be described linearly, *e.g.* in the range of 0.065–0.32 mm s^{-1}. However, with the increase of the velocity, the rate of increase slows down and eventually displays a trend of saturation, *i.e.* the fluorescence intensity will not increase with the flow velocity. In this case, the sensitivity of the measurement is greatly reduced for high flow velocity. For this reason, the calibration curve in Fig. 5 is only suitable for velocity measurement within the calibrated velocity range of 0.065–3.5 mm s^{-1} to warrant the sufficient sensitivity of the measurement. The calibration polynomial eqn. (5) should not be extrapolated outside the calibration data range.

Verification in pressure driven flow

To validate the calibration curve for the velocity measurement, we use the same way of measuring the calibration curve to verify LIFPA for measuring the flow velocity with the calibration curve. For each given flow rate, we measure the fluorescence intensity and the corresponding flush time. The measured u based on the flush time measurement *versus* its corresponding I_f is also shown in Fig. 5 with symbols of unfilled circle for comparison. The time duration between the calibration and the verification measurement was 2 h. The coefficient of determination between the calibration curve and the measured data for verification, *i.e.* R-squared value, is 0.99. The error bar that is the standard deviation obtained from more than 20 events, is also shown in Fig. 5. The error bar increases with velocity. However, the relative standard deviation does not increase with the velocity. The average relative standard deviation is 3.2% at the highest velocity of U = 3.5 mm s^{-1}, and 3.7% at the lowest velocity of U = 0.065 mm s^{-1}. The error is random and its source could come from the optical detector, pump pressure, laser power fluctuation and detection point temperature fluctuation. Fig. 5 demonstrates that, for each fluorescence intensity value, the measured velocity matches very well with the calibration curve and confirms that the calibration curve can be used to measure the flow velocity in the microchannel.

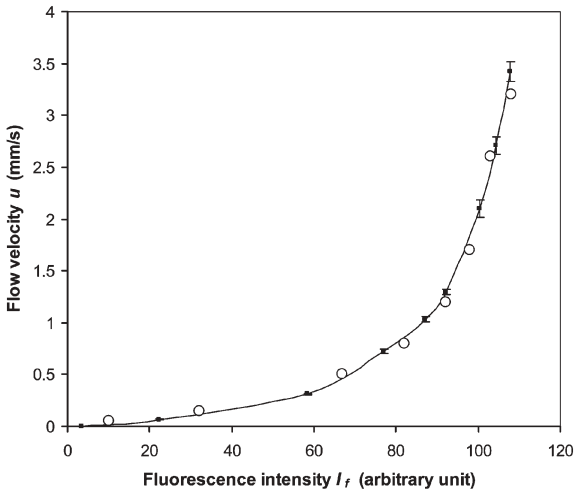

Fig. 5 Relationship between flow velocity u and fluorescence intensity I_f. (■) represents the measured u using the flush time for calibration between flow velocity and fluorescence intensity. The laser power is 700 mW and the measuring spot size is 0.18 nL with focusing beam sheet 25 μm in thickness. The same laser power and spot size is used for all following figure captions. Line (—) is calibration curve of the non-linear fitting based on the measured u and I_f. (○) denotes the measured u using flush time two hours later after the calibration to verify the calibration curve for LIFPA. The error bar is the standard deviation. The average relative standard deviation is 3.2% at the highest velocity of U = 3.5 mm s^{-1}, and 3.7% at the lowest velocity of U = 0.065 mm s^{-1}.

Measurement of EOF

The calibration curve can be applied to measure flow velocity not only in pressure driven flow, but also in EOF or the combination of pressure driven and EOF as long as the velocity is within the range of the calibration curve. Here we will demonstrate a case of the application of LIFPA to EOF.

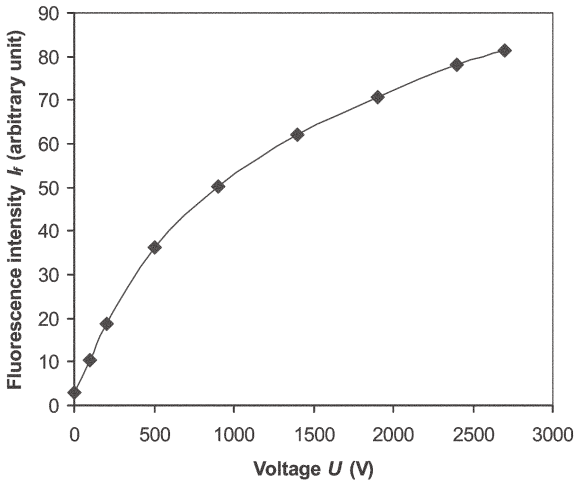

Fig. 6 Relationship between fluorescence intensity and voltage for electroosmotic flow. The figure shows that the fluorescence intensity increases with voltage in a similar manner as fluorescence intensity increases with flow velocity.

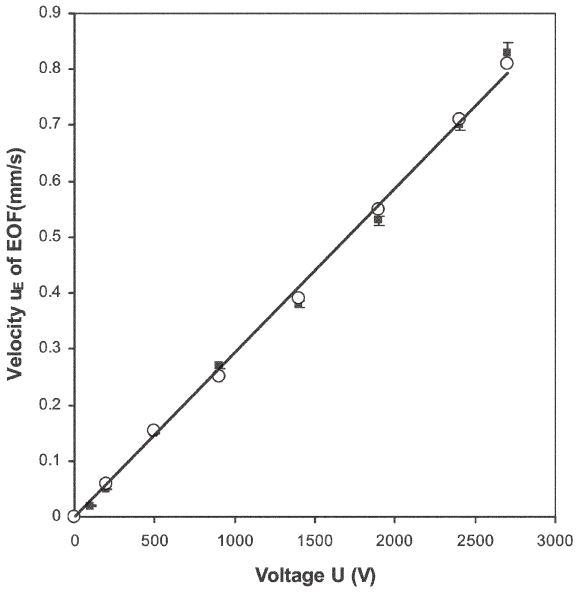

Fig. 7 Relationship between velocity of electroosmotic flow and voltage supplied at the inlet and outlet of the microchannel. (■) represents the calculated velocity of electroosmotic flow with eqn. (5) from measured fluorescence intensity. (○) denotes the measured velocity of electroosmotic flow using flush time for verification. The error bar is the standard deviation.

For EOF, the voltage was used to drive the flow. Similar to Fig. 3 in pressure driven flow, for a given voltage U between the electrodes from the inlet and outlet of the microchannel, I_f was also a constant in EOF. We ran different voltages ranging from 0 to 2700 V, and measured the corresponding values of I_f. The measured relationship between I_f and U is displayed in Fig. 6, which clearly shows that I_f increases with voltage, similar to the relation between fluorescence intensity and flow velocity. This is expected, since the flow velocity u_E of EOF increases with electric field intensity, *i.e.* voltage here.

Using eqn. (5) we can easily calculate the flow velocities u_E of the EOF in Fig. 6 corresponding to different values of voltage. The corresponding relationship between flow velocity and voltage is shown in Fig. 7 as filled square symbols. Apparently u_E linearly increases with voltage, indicating that the mobility was constant. The measurement is also extrapolated to the lowest $u_E = 0.021$ mm s^{-1} and it fits very closely to the linear relation between u_E and voltage, probably because of the nearly linear relationship between flow velocity and fluorescence intensity at low velocity range. The error bar is also shown in Fig. 7. The error bar is obtained from more than 20 events during 10 minutes. The highest u_E is within the calibration range and its relative deviation is 2.5%. The relative deviation of the lowest EOF u_E is 2.8%. The error could also results from the voltage fluctuation of power supplier.

To validate the estimated velocity in Fig. 7 from the calibration curve in Fig. 5, the flush time measurement was again used to measure flow velocity u_E of EOF for different voltage. To measure the flush time, we switched on the high voltage power supplier between inlet A and outlet electrodes for a given voltage, and ran the experiment over a sufficient amount of time to fill the dye solution from the inlet A to the outlet. After filling, we turned the electricity off between the inlet A and outlet, and turned on the pump connected to the inlet B for about 1 s to provide an injection of buffer solution slug without dye. Then the pump was quickly turned off. The connection between the inlet A and outlet was turned on immediately again at the same voltage. We count the time as the starting time. When the buffer slug arrived at the detecting point, there was a dip in the trace of I_f. Through this process, we can minimize the usage of the pure buffer solution to reduce the influence of EOF mobility difference between the dye and pure buffer solutions, if any.

The measured u_E using flush time is represented in Fig. 7 as unfilled circles. The *R*-squared value between the velocities obtained from the calibration curve and flush time measurement is 0.99. Fig. 7 demonstrates that the velocity calculated using eqn. 5 matches very well with the measured u_E. Therefore, the calibration curve for LIFPA can be used to calculate velocity with the measured fluorescence intensity regardless of whether flow is pressure driven or EOF.

Discussion

The exponential relationship between fluorescence intensity and flow velocity is normally not a favorable scaling for experimental measurement, since at high velocity the sensitivity is relatively low. However, the calibration curve of Fig. 5 between fluorescence intensity and flow velocity is similar to that between voltage and flow velocity of Hot-Wire Anemometer widely used in fluid mechanics.[50] We should not use the range near saturation between flow velocity and fluorescence intensity, where the sensitivity is poor. The current work uses high concentration dye to increase the photobleaching for the dynamic range of 0.065–3.5 mm s^{-1} with sufficient sensitivity. If the dye concentration has to be low and the laser power is also low, a dye with stronger photobleaching (*e.g.* Carbostyril 124) should be selected and the laser beam should be focused to a fine cylindrical spot instead of the sheet

to increase laser intensity, in order to keep the high sensitivity. In the high velocity range of the pressure driven flow, the ratio of velocity to fluorescence intensity is 0.2. The deviation of fluorescence intensity for the highest velocity is 0.13. The corresponding relative velocity deviation caused by the deviation of fluorescence intensity is about 2.9%. For EOF, since the maximum velocity is only 0.81 mm s^{-1}, the sensitivity is relatively high, and the velocity deviation of the EOF caused by the fluorescence deviation is 2.3%. If all parameters (*e.g.* dye concentration, laser intensity and *etc.*) that can cause the change of fluorescence intensity, including the optical setup, are kept constant, the calibration curve should be stable and independent of time.

Another issue that needs to be addressed is that the low velocity limitation is not zero for the dynamic range, even though the relationship between fluorescence intensity and flow velocity is nearly linear. When the flow is slow enough that it is comparable to the diffusion time of the dye molecule into and out of the laser focus, this technique will no longer be able to tell what the flow velocity is as the extremely low limit is approached. (The present method is not intended to measure flow velocity, where Brownian motion is important since it is very difficult to measure that lower limit with flush time. For velocity near the region of Brownian motion, fluorescence recovery after photobleaching (FRAP) should be considered.[51,52]) In the current work, the calibrated lowest velocity is 0.065 mm s^{-1}. The velocity deviation is not high at low velocity range, since the relationship between flow velocity and fluorescence intensity is nearly linear and the sensitivity is very high at low velocity (the curve slope of velocity to fluorescence intensity is 0.0060). The standard deviation of the fluorescence intensity is 0.0025, which causes a relative velocity deviation of 3.5% for pressure driven flow and 1.6% for EOF at the lowest velocity respectively.

At relatively low velocity range, the relation is approximately linear as shown in Fig. 5 and Ricka's work.[48] The linear range, dynamic range and sensitivity can be increased by enhancing photobleaching. For microfluidics in bioanalytical systems, flow velocity is often in the range of 10 μm s^{-1}–10 mm s^{-1}. This can easily be measured with sufficiently high sensitivity, if we focus the laser to a cylindrical spot[46] instead of the sheet in the present work for a laser beam with power of several hundreds of milliWatts. The present work used a laser sheet for a different purpose, and thus reduced the laser intensity in the detecting probe volume. We can also use other dyes with strong photobleaching to increase the sensitivity.

Although photobleaching has been applied to measure flow velocity with different mechanisms[39–44] as mentioned in the introduction, LIFPA seems to be a novel method and shows several advantages. For instance, the two points based method in Pittman *et al.*[44] can only measure the bulk flow velocity and the temporal resolution is limited, since it has to wait for the bleached dye slug to translate from the laser beam to the detecting point. Since the current method is based on a single point measurement, it can measure velocity distribution in the transverse direction with high spatial resolution; the velocity is directly measured with the calibration curve, and thus also has high temporal resolution. The response time of LIFPA is determined by the fluorescence photobleaching kinetics or decay time constant, which can be several hundreds of microseconds.[46] Therefore the temporal resolution of LIFPA could be in the order of milliseconds. The decay time constant can be further reduced by enhancing photobleaching.

Although the present work only introduces the measurement of local bulk flow velocity, the spatial resolution of LIFPA could be very high because it is based on a molecular tracer. Since the waist of the laser beam is limited by diffraction and can be focused to even less than 1 μm in diameter, the spatial resolution for a point measurement with 1 μm spatial resolution is possible. LIFPA could also be applied to measure a two-dimensional velocity field with a camera.[48] Due to the fast response, LIFPA can be used to measure instantaneous flow velocity and monitor the flow velocity online, when the signal of fluorescence intensity is calculated by a computer using the calibration eqn. (5). Fig. 3 is actually an example of online velocity monitoring.

LIFPA is based on the one to one relationship between fluorescence intensity and flow velocity. Therefore, any other parameter that has an effect on fluorescence intensity should be avoided. For the velocity measurement, the dye solution should be kept constant, since fluorescence intensity strongly depends on the dye's concentration. Fluid temperature should also be kept constant since fluorescence intensity also depends on the temperature.[53] Buffer solution should also be kept constant, if fluorescence intensity depends also on pH.[49]

The principle of LIFPA is not limited to the laser, and can also be applied to other light sources, as long as the photobleaching becomes sufficiently strong for the measurement to have sufficient sensitivity. In addition to the flush time measurement, any other method of velocity measurement can also be used to measure flow velocity for calibration.

Compared with the work of Ricka,[48] which uses similar method with photobleaching, the theoretical model presented in this paper is very simple and would be helpful for readers without advanced mathematics background. The flow velocity in the calibration curve of the current work has also been expanded one order higher (note the laser power is less than half of that used in Ricka's work). The main reason is the use of high dye concentration. Compared with other methods using photobleaching to measure flow velocity, the current method measures fluorescence intensity only at one spatial point, and does not need to measure different downstream changes in fluorescence intensity, and thus, has high spatial and temporal resolution simultaneously and is easy to use. However, the current method requires calibration.

Summary and conclusion

We have demonstrated a novel and non-intrusive anemometer based on laser-induced fluorescence photobleaching for microfluidic devices. A simplified model is used to describe the mechanism of the anemometer. A calibration curve between fluorescence intensity and flow velocity is initially required for this method. The calibration curve can be obtained with any method, such as the measurement of a fluid flush time. With the calibration curve, the flow velocity can be easily and directly obtained from the measured fluorescence intensity signal for both pressure driven flow and electroosmotic flow.

The method is validated to match very well with the measured velocity acquired with the measurement of the flush time.

Acknowledgements

The author thanks Professor Koochesfahani, M. M. from Michigan State University for discussion on phobobleaching.

G. R. Wang
CFD Research Corporation, 215 Wynn Dr, Huntsville, AL35805, USA. E-mail: guirenwang@yahoo.com

References

1 D. J. Beebe, G. A. Mensing and G. M. Walker, *Annu. Rev. Biomed. Eng.*, 2002, **4**, 261–86.
2 D. R. Reyes, D. Iossifidis, P. Auroux and A. Manz, *Anal. Chem.*, 2002, **74**, 2623–36.
3 L. Bousse, C. Cohen, T. Nikiforov, A. Chow, A. R. Kopf-Sill, R. Dubrow and J. W. Parce, *Annu. Rev. Biophys. Biomol. Struct.*, 2000, **29**, 155–81.
4 S. A. Sundberg, A. Chow, T. Nikiforov and H. G. Wada, *Drug Discovery Today*, 2000, **5**, Suppl., S92–103.
5 K. D. Lukacs and J. W. J. Jorgenson, *High Resolut. Chromatogr. Chromatogr. Commun.*, 1985, **8**, 407–411.
6 S. Terabe, K. Otsuka, K. Ichikawa, A. Tsuchiya and T. Ando, *Anal. Chem.*, 1984, **56**, 111–113.
7 L. Tang and C. O. Huber, *Talanta*, 1994, **41**, 1791.
8 T. Tsuda, S. Kitagawa, R. Dadoo and R. N. Zare, *Bunseki Kagaku*, 1997, **46**, 409–414.
9 J. Moorthy, C. Khoury, J. S. Moore and D. J. Beebe, *Sens. Actuators, B–Chemical*, 2001, **75**, 223–229.
10 F. Bianchi, F. Wagner, P. Hoffmann and H. H. Girault, *Anal. Chem.*, 2001, **73**, 829–836.
11 T. Tsuda, K. Nomura and G. Nakagawa, *J. Chromatogr.*, 1982, **248**, 241.
12 Y. Walbroehl and J. W. Jorgenson, *Anal. Chem.*, 1986, **58**, 479–481.
13 W. J. Lambert and D. L. Middleton, *Anal. Chem.*, 1990, **62**, 1585–1587.
14 J. E. Sandoval and S. M. Chen, *Anal. Chem.*, 1996, **68**, 2771–2775.
15 M. Hayes and A. Ewing, *Anal. Chem.*, 1992, **64**, 512–516.
16 B. A. Williams and G. Vigh, *Anal. Chem.*, 1997, **69**, 4445–4451.
17 J. P. Preisler and E. S. Yeung, *Anal. Chem.*, 1996, **68**, 2885–2889.
18 K. D. Altria and C. F. Simpson, *Chromatographia*, 1987, **24**, 527–532.
19 O. T. Guenat, D. Ghiglione, W. E. Morf and N. F. de Rooij, *Sens. Actuators, B–Chemical*, 2001, **72**, 273.
20 Y. Liu, D. O. Wipf and C. S. Henry, *Analyst*, 2001, **126**, 1248–1251.
21 B. J. Wanders, T. A. A. M. van de Goor and F. M. J. Everaerts, *Chromatogr. A*, 1993, **652**, 291–294.
22 X. Huang, M. J. Gordon and R. N. Zare, *Anal. Chem.*, 1988, **60**, 1837–1838.
23 C. S. Lee, D. McManigill, C. T. Wu and B. Patel, *Anal. Chem.*, 1991, **63**, 1519–1523.
24 G. Ocvirk, M. Munroe, T. Tang, R. Oleschuk, K. Westra and D. J. Harrison, *Electrophoresis*, 2000, **21**, 107–115.
25 L. E. Locascio and C. E. Perso, *J. Chromatogr. A*, 1999, **857**, 275–284.
26 R. L. Chien and J. C. Helmer, *Anal. Chem.*, 1991, **63**, 1354–1361.
27 A. van de Goor, B. J. Wanders and F. M. Everaerts, *J. Chromatogr.*, 1989, **470**, 95–104.
28 J. C. Reijenga, G. V. A. Aben, T. Verheggen and F. M. Everaerts, *J. Chromatogr.*, 1983, **260**, 241–254.
29 Y. G. Gu and D. Q. Li, *J. Colloid Interface Sci.*, 2000, **226**, 328–339.
30 D. Ross, T. J. Johnson and L. E. Locascio, *Anal. Chem.*, 2001, **73**, 2509–2515.
31 J. I. Molho, A. E. Herr, B. P. Mosier, J. G. Santiago, T. W. Kenny, R. A. Brennen, G. B. Gordon and B. Mohammadi, *Anal. Chem.*, 2001, **73**, 1350–1360.
32 B. Manz, P. Stilbs, B. Jonsson, O. Soderman and P. T. Callaghan, *J. Phys. Chem.*, 1995, **99**, 11297.
33 D. H. Wu, A. Chen and C. S. Johnson, *J. Magn. Reson., Ser. A*, 1995, **115**, 123.
34 U. Tallarek, E. Rapp, T. Scheenen, E. Bayer and H. VanAs, *Anal. Chem.*, 2000, **72**, 2292–2301.
35 B. R. Locke, M. Acton and S. J. Gibbs, *Langmuir*, 2001, **17**, 6771–6781.
36 S. Devasenathipathy, J. G. Santiago and K. Takehara, *Anal. Chem.*, 2002, **74**, 3704–3713.
37 J. G. Santiago, S. T. Wereley, C. D. Meinhart, D. J. Beebe and R. J. Adrian, *Exp. Fluids*, 1998, **25**, 316–319.
38 E. B. Cummings, *AIAA J.*, 2001, 2001–1163.
39 C. A. Monnig and J. W. Jorgenson, *Anal. Chem.*, 1991, **63**, 802–807.
40 A. W. Moore and J. W. Jorgenson, *Anal. Chem.*, 1993, **65**, 3550–3560.
41 B. P. Mosier, J. I. Molho and J. G. Santiago, *Exp. Fluids*, 2002, **33**, 545–554.
42 K. F. Schrum, J. M. Lancaster, S. E. Johnston and S. D. Gilman, *Anal. Chem.*, 2000, **72**, 4317–4321.
43 J. L. Pittman, K. F. Schrum and S. D. Gilman, *Analyst*, 2001, **126**, 1240–1247.
44 J. L. Pittman, C. S. Henry and S. D. Gilman, *Anal. Chem.*, 2003, **75**, 361–370.
45 S. Devasenathipathy and J. G. Santiago, *Micro- and Nano-Scale Diagnostic Techniques,* ed. K.S. Breuer, Springer Verlag, New York, in press, 2003.
46 G. R. Wang and H. E. Fiedler, *Exp. Fluids*, 2000, **29**, 257–264.
47 H. E. Fiedler and G. R. Wang, *Deutsches Patent, 19838344.4*, 1998, Germany.
48 J. Ricka, *Exp. Fluids*, 1987, **5**, 381–384.
49 M. M. Koochesfahani, *Experiments on turbulent mixing and chemical reaction in a liquid mixing layer*, PhD Thesis, Caltech, Pasadena, CA USA, 1984.
50 R. J. Goldstein, *Fluid Mechanics Measurements*, 1983, Hemisphere Publishing Corp.
51 J. White and E. Stelzer, *Trends Cell Biol.*, 1999, **9**, 61–65.
52 B. Storrie, R. Pepperkok, E. Stelzer and T. E. Kreis, *J. Cell Science*, 1994, **107**, 1309–1319.
53 D. A. Walker, *J. Phys E: Sci. Instrum.*, 1987, **20**, 217–224.

